Research Article

Journal of Environmental Nanotechnology

Structural, Morphological, and Photocatalytic Studies of Co-Doped MoO_3 on SiO_2: A Multifunctional Material for Environmental Remediation

S. Boobesh[1], P. Sanjeevi[1], G. Kalpana[2], C. Sivaraj[3] and M. Elango[1*]

[1]Department of Physics, PSG College of Arts and Science, Coimbatore, TN, India
[2]Department of Science and Humanities, Tamil Nadu College of Engineering, Coimbatore, TN, India
[3]Department of Mathematics, PSG College of Arts and Science, Coimbatore, TN, India
Received: 12.09.2024 Accepted: 15.11.2024 Published: 30.12.2024
*elango@psgcas.ac.in

ABSTRACT

Molybdenum trioxide is a versatile material widely studied for its unique structural, electronic, and optical properties, making it suitable for applications in catalysis, photocatalysis, energy storage, and environmental remediation. In this study, the structural and functional properties of undoped and Co-doped MoO_3 on SiO_2 were systematically investigated through XRD, FESEM, TEM, UV-Vis, FTIR, EDS, and dye degradation experiments. The XRD analysis revealed the crystalline structure and lattice distortions induced by Co doping, while FESEM and TEM demonstrated the morphological evolution, including agglomeration and increased surface roughness. Optical studies using UV-Vis spectroscopy showed a bandgap narrowing upon doping, enhancing photocatalytic activity. The FTIR spectra highlighted shifts in vibrational modes, confirming structural modifications due to doping. The EDS analysis confirmed the successful incorporation of cobalt into the MoO_3 matrix. The photocatalytic efficiency of 6% Co-doped MoO_3 was evaluated using Isolan Black dye, with results showing significant degradation within 60 min. Based on the findings, the Co-doped MoO_3 on SiO_2 can be claimed as an efficient material for environmental and catalytic applications.

Keywords: Nano Co-doped MoO_3 on SiO_2; Physicochemical characterization; Photocatalytic degradation; Isolan Black dye.

1. INTRODUCTION

Molybdenum trioxide is a versatile transition metal oxide drew attention for its unique structural, electronic, and optical properties. It crystallizes predominantly in the orthorhombic phase, characterized by layered arrangements of MoO_3 octahedra, which offer high surface areas and tunable electronic structures. These attributes make MoO_3 highly suitable for applications in catalysis, gas sensing, energy storage, and environmental remediation (Rajesh *et al.* 2014). Cobalt doping in MoO_3 further enhances its performance by altering its electronic structure, introducing defects, and narrowing its bandgap, thus increasing its activity under visible light.

Co-doping of MoO_3/ SiO_2 has proven effective in enhancing photocatalytic and adsorption capacities, as it promotes charge carrier separation and reactive oxygen species (ROS) generation. These advancements position Co-doped MoO_3 as a promising candidate for removing organic pollutants and dyes from industrial wastewater (Chen *et al.* 2022).

2. MATERIALS AND METHODS

2.1 Materials

The analytical grade precursor chemicals hexa ammonium hepta molybdate $(NH_4)_6Mo_7O_{24}.H_2O$, HNO_3, liquid ammonia purchased from Merck, India were used without any further purification.

2.2 Preparation Protocol

SiO_2 spheres was synthesized using the Stöber process. Initially, 1 g of cetyltrimethylammonium bromide (CTAB) was dissolved in a 1:2 ethanol-to-water mixture. Once fully dissolved, 0.8 mL of tetraethyl orthosilicate (TEOS) was added to the solution, stirred continuously for 2 hours. The white precipitate formed was collected through centrifugation and thoroughly washed multiple times with ethanol and water. The resulting precipitate was dried in a hot air oven at 100 °C for 12 hours. The prepared SiO_2 particles were preserved for further characterization. The preparation of undoped MoO_3 on SiO_2 and cobalt-doped MoO_3 on SiO_2 was carried out using a facile wet-chemical method. Initially, 0.3 g of synthesized SiO_2 particles were dispersed in 100

mL of deionized water under constant stirring to form a stable colloidal solution. Subsequently, 0.2 mol of a molybdate precursor hexa ammonium hepta Molybdate and the required amount of cobalt precursor Cobalt Nitrate $Co(NO_3)_2$ (based on the desired doping concentration) were added to the solution, followed by stirring for 30 min to ensure complete dissolution. To the resulting mixture, 25 mL of concentrated nitric acid was added dropwise. After another 30 min of stirring, ammonia was added gradually as a precipitating agent until the pH of the solution reached 11.

The homogeneous solution was stirred continuously at 85 ℃ for 3 hours to facilitate the formation of precipitates. The obtained precipitate was aged at room temperature for 4 hours to improve crystallinity and uniformity. The precipitate was then collected *via* centrifugation at 3000 rpm for 10 min and thoroughly washed several times with acetone and ethanol to remove impurities. The washed precipitate was dried in an oven at 120 ℃ for 24 hours. The dried powder was subsequently calcined at 500 ℃ for 3 hours to achieve the desired crystalline phase of MoO_3.

The same protocol was followed for samples with 6% and 9% cobalt doping concentrations. The resulting samples were analyzed to investigate their structural, optical, and photocatalytic dye degradation properties. The optimized preparation conditions ensured homogeneity and reproducibility of the materials for further characterization.

2.3 Sample Characterization

The prepared samples were characterized using a comprehensive tool to examine their structural, textural, surface-chemistry and morphological properties. The structural analysis was done using X-ray diffraction (XRD), high-resolution transmission electron microscopy (HR-TEM). The XRD patterns were obtained with an X'Pert Pro X-ray diffractometer employing a CuK_α anode (λ = 1.5406 Å) operated at 40 KV and a scanning step rate of 0.02°/min. TEM micrographs and selected area electron diffraction (SAED) pattern were captured using JEOL-JEM (2010) microscope to provide the valuable insights into the 3D-morphology, topography, and lattice orientations. Fourier-transform infrared spectral analysis was made using BRUKER Alpha spectrometer employing KBr pellet technique recording a wavelength range of 400-4000 cm^{-1}. Finally, the surface morphology was examined using a TESCAN MIRA-3 scanning electron microscope equipped with an energy-dispersive X-ray (EDX) detector to provide both morphological and compositional data. The photocatalytic performance of the synthesized nanoparticles was evaluated by employing them for the degradation of Isolan Black dye at a concentration of 60 ppm over various time intervals.

3. RESULTS AND DISCUSSION

3.1 XRD Analysis

The X-ray diffraction (XRD) patterns for undoped and Co-doped MoO_3 on SiO_2 (Fig. 1) confirm the crystallinity and structural modifications induced by doping. The undoped MoO_3 exhibits sharp diffraction peaks, indicative of a well-defined orthorhombic structure. Upon doping with cobalt at varying concentrations (3%, 6%, and 9%), slight peak shifts and broadening are observed, reflecting lattice distortions and strain caused by the incorporation of Co ions into the MoO_3 lattice (Kumar *et al.* 2020). The average particle size was calculate using Debye Scherer formula and it was found at the undoped MoO_3 has a particle size of undoped was 46 nm whereas its cobalt doped variants ranges from 64 nm, 49nm and 53 nm for the

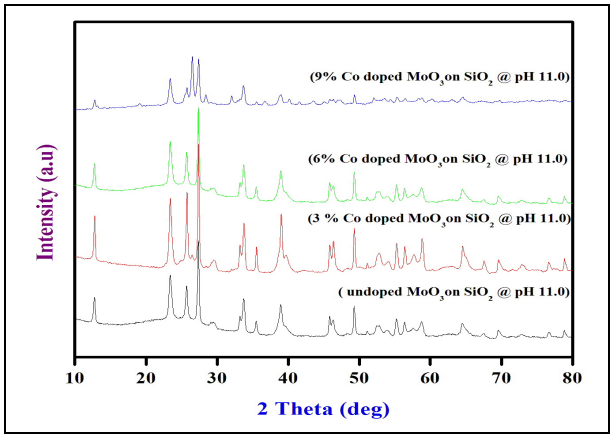

Fig. 1: XRD spectra of undoped MoO_3 on SiO_2 nanoparticles and 3%, 6% and 9% Cobalt-doped MoO_3 on SiO_2

At higher doping concentrations, secondary peaks associated with Co species emerge, suggesting phase separation or the saturation of cobalt in the lattice. These structural modifications correlate with increased defect density and surface roughness, which can improve photocatalytic properties while potentially affecting material stability. (Wang *et al.* 2021).

3.2 FESEM Analysis

Fig 2 shows the field-emission scanning electron microscopy (FESEM) images that reveal the morphological differences between undoped (a) and Co-doped MoO_3. The undoped sample shows uniformly distributed granular particles with smooth surfaces and well-defined boundaries, indicative of high crystallinity. In contrast, Co doping induces significant agglomeration and surface roughness, particularly at 6% and 9% doping concentrations (Zhou *et al.* 2021). The particle size calculate from the SEM were found to range between 50 – 60 nm.

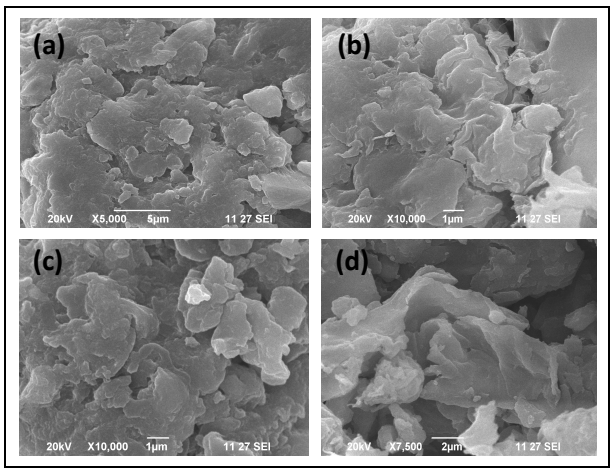

Fig. 2: FESEM images of (a) undoped MoO_3 on SiO_2 (b) 3% Co Doped MoO_3 on SiO_2 (c) 6% Co Doped MoO_3 on SiO_2 (d) 9% Co Doped MoO_3 on SiO_2

The observed agglomeration in the doped samples results from lattice strain and increased inter-particle interactions due to Co incorporation. These morphological changes enhance the surface area and create additional active sites, making the material suitable for catalytic applications. However, excessive doping may compromise structural stability (Elango *et al.* 2018).

3.3 TEM Analysis

High-resolution transmission electron microscopy (HRTEM) images shown in Fig. 3 highlight the structural differences between undoped and 6% Co-doped MoO_3. The undoped sample exhibits well-dispersed particles with distinct edges and minimal aggregation, confirming its crystalline nature. In contrast, the doped sample shows clustered particles with irregular shapes and rougher textures, reflecting lattice distortions caused by cobalt doping (Li *et al.* 2020).

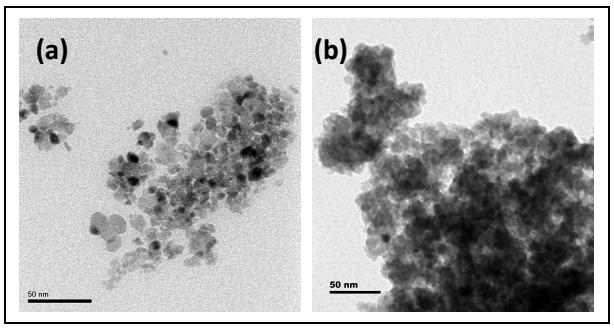

Fig. 3: TEM images of (a) undoped MoO_3 on SiO_2 (b) Co Doped MoO_3 on SiO_2

The increased agglomeration and defect density in the doped sample enhance the functional properties of the material, such as catalytic and adsorption activities. However, optimizing doping levels is essential to balance these benefits with structural stability (Chen *et al.* 2022).

3.4 UV-Vis Analysis

Fig. 4 illustrates UV-Vis absorption spectra of the Co-doped MoO_3 samples that demonstrate their enhanced photocatalytic property under visible light. The undoped MoO_3 primarily absorbs in the UV region, while cobalt doping induces a redshift, narrowing the bandgap and enabling better absorption of visible light. This shift is attributed to the introduction of localized energy states by Co ions (Gunasekaran *et al.* 2021).

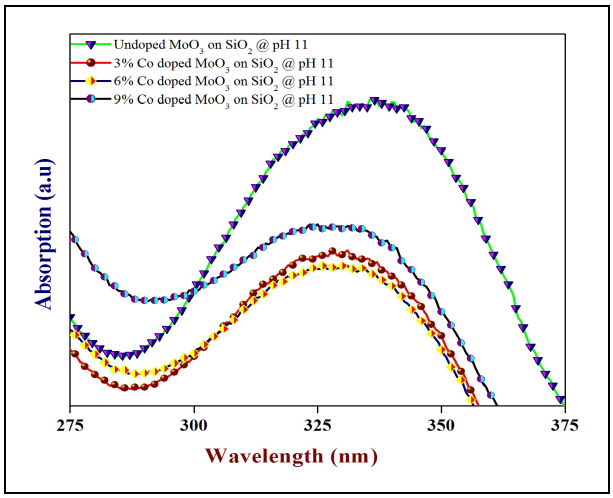

Fig. 4: UV Visible spectrograms of undoped MoO_3 on SiO_2 nanoparticles and 3%, 6% and 9% Cobalt doped MoO_3 on SiO_2

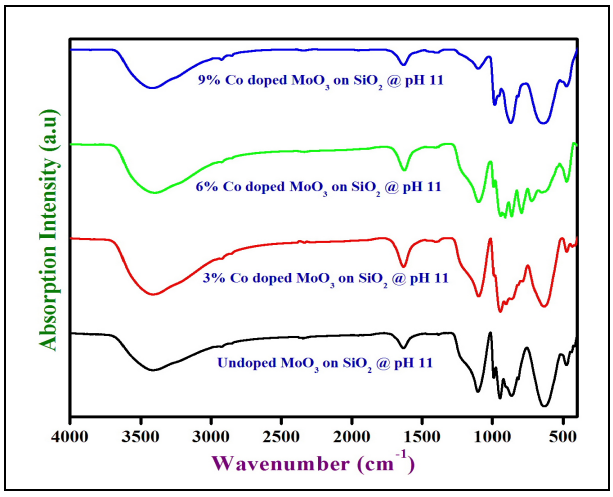

Fig. 5: Fourier Transform IR spectrograms of undoped MoO_3 on SiO_2 nanoparticles and 3%, 6% and 9% Cobalt doped MoO_3 on SiO_2

These optical changes directly enhance the photocatalytic performance of the material, as demonstrated by its ability to degrade dyes effectively under visible light. This makes Co-doped MoO_3 a

suitable material for environmental remediation (Kumar *et al.* 2021).

4.5 FTIR Analysis

Fourier-transform infrared (FTIR) spectroscopy (Fig 5) highlights the vibrational modes of MoO_3 and the structural changes induced by cobalt doping. The undoped MoO_3 exhibits characteristic Mo=O and Mo–O–Mo vibrations in the fingerprint region around 500 – 600 cm^{-1}, confirming its octahedral structure. Upon doping, these peaks shift slightly, reflecting distortions in the MoO_3 lattice due to Co incorporation (Tariq *et al.* 2020).

The intensity reduction in the hydroxyl (-OH) stretching region with increasing doping concentrations suggests stronger interactions between MoO_3 and SiO_2 or reduced surface hydroxylation. These changes improve the catalytic properties of the material by increasing defect density and reactive sites (Rajesh *et al.* 2014).

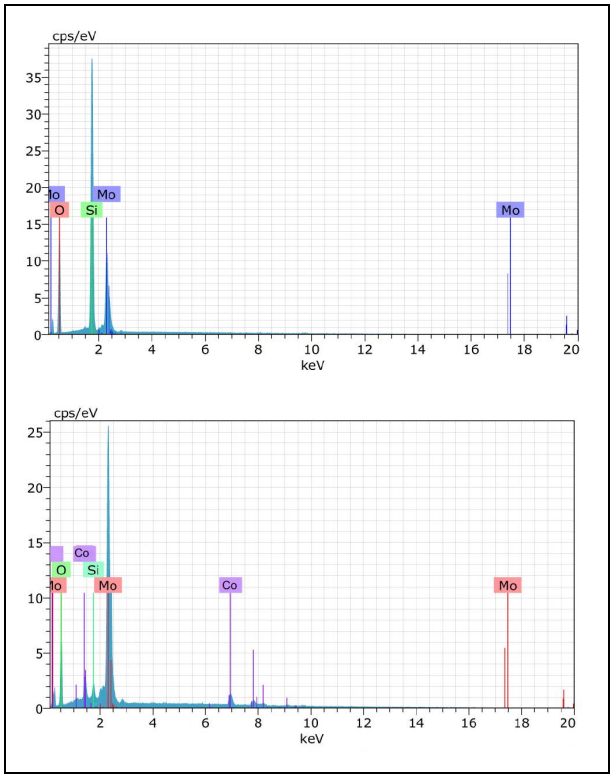

Fig. 6: Energy-dispersive X-ray spectroscopy of (a) undoped MoO_3 on SiO_2 (b) Co Doped MoO_3 on SiO_2

4.6 EDS Analysis

Fig 6 depict the energy-dispersive X-ray spectroscopy (EDS) of prepared samples which confirms the elemental composition of undoped and Co-doped MoO_3. The undoped sample shows peaks for Mo and O, consistent with its stoichiometry. In the doped samples, additional peaks for Co appear, confirming successful doping. The relative intensity of the Co peaks increases with doping concentration.

This elemental mapping demonstrates the uniform distribution of cobalt within the MoO_3 lattice. The incorporation of cobalt ions enhances the functional properties of the material by introducing defects and modifying the electronic structure, essential for catalytic and adsorption applications (Wang *et al.* 2021).

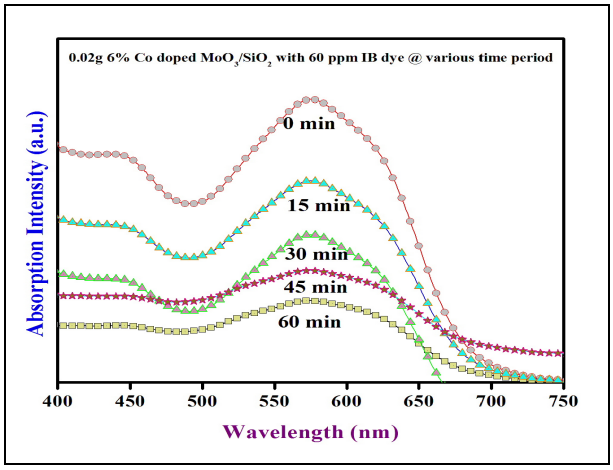

Fig. 7: Dye degradation analysis: degradation of Isolan Black dye using Co doped MoO_3/SiO_2 for various time periods

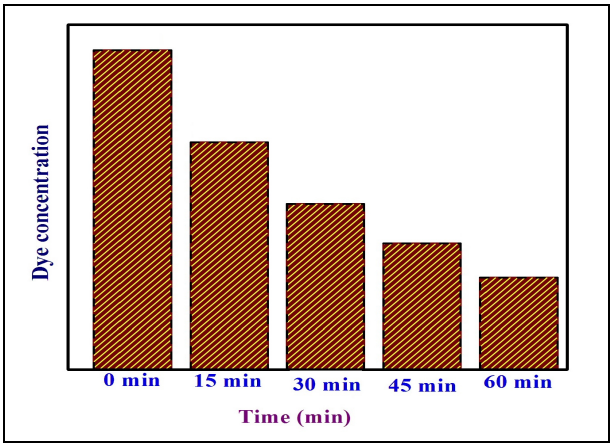

Fig. 8: Degradation level for various duration (bar Chart representation)

4.7 Dye Degradation

The Isolan Black (IB) dye was selected for the photocatalytic degradation investigation because of its widespread industrial application and its designation as a recalcitrant azo dye, characterized by significant stability and resistance to standard wastewater treatment methods. Its intricate aromatic configuration and azo (-N=N-) linkages render it a persistent environmental contaminant. The dye's significant absorption in the

visible band (600–700 nm) renders it suitable for assessing visible-light-driven photocatalytic systems such as Co-doped MoO_3. The successful degradation of IB dye illustrates the photocatalyst's efficacy in decomposing stable contaminants, underscoring its potential for industrial wastewater treatment and environmental remediation applications.

Since the physiochemical properties of 6 % Co doped MoO_3 on SiO_2 has promising and appreciable towards dye degradation, The photocatalytic activity of only 6% Co-doped MoO_3 was evaluated through the degradation of Isolan Black dye. The UV-Vis absorption spectra (Fig 7) show a progressive reduction in the characteristic absorption peak (~600–700 nm) of the dye over 60 min, indicating significant dye degradation. The bar chart showed in Fig 8, quantifies this reduction, revealing a near-linear decrease in dye concentration over time (Kumar *et al.* 2021).

The efficient degradation is attributed to the enhanced photocatalytic activity of Co-doped MoO_3, which narrows the bandgap and facilitates charge separation, generating reactive oxygen species. This makes it a promising material for wastewater treatment, particularly in removing organic pollutants (Chen *et al.* 2022). This structured analysis highlights the potential of Co-doped MoO_3 for multifunctional applications, particularly in environmental remediation and catalysis.

5. CONCLUSION

The systematic investigation of undoped and Co-doped MoO_3 on SiO_2 has provided valuable insights into the structural, optical, and functional enhancements introduced by cobalt doping. The XRD and FTIR analyses confirmed lattice distortions and structural modifications, while FESEM and TEM revealed morphological changes, including increased surface roughness and particle agglomeration at higher doping levels. UV-Vis spectroscopy demonstrated that cobalt doping narrows the bandgap of MoO_3, enabling better absorption of visible light and enhancing photocatalytic performance. The EDS analysis confirmed successful incorporation and uniform distribution of cobalt within the MoO_3 lattice.

The degradation of Isolan Black dye using 6% Co-doped MoO_3 demonstrated the high photocatalytic efficiency of the material, attributed to the generation of reactive oxygen species and improved charge separation. These results highlight the potential of Co-doped MoO_3 as a multifunctional material for applications in environmental remediation and catalysis. Future studies can focus on optimizing doping concentrations and exploring additional functional properties to enhance the performance and versatility of this material.

FUNDING

This research received no specific grant from any funding agency in the public, commercial, or not-for-profit sectors.

CONFLICTS OF INTEREST

The authors declare that there is no conflict of interest.

REFERENCES

Chen, J., Wang, L. and Huang, S., Enhanced photocatalytic performance of cobalt-doped molybdenum trioxide for organic pollutant degradation, *Mater. Des., 215*, 110091 (2022). https://doi.org/10.1016/j.matdes.2022.110091

Elango, M., Kalpana, G., Varuna, J. and Sanjeevi, P., Influence of Mg concentration on structural, morphological and optical properties of nanoceria, *Ceram. Int.*, 44(10), 11820-11827 (2018). https://doi.org/10.1016/j.ceramint.2018.03.269

Li, M., Dong, Q. and Xu, F., High-resolution TEM analysis of transition metal-doped MoO_3: Structural insights and defect mechanisms, *Mater. Des, 190*, 107810 (2020). https://doi.org/10.1016/j.matdes.2020.107810

Gunasekaran, S., Marnadu, R., Thangaraju, D., Chandrasekaran, J., Hegazy, H. H., Somaily, H. H., Durairajan, A., Valente, M.A., Elango, M., Vasudeva Reddy and Minnam Reddy, Development of n-MoO_3@MoS_2/p-Si heterostructure diode using pre-synthesized core@shell nanocomposite for efficient light harvesting detector application, *Mater. Sci. Semicond. Process.*, 135, 106097 (2021). https://doi.org/10.1016/j.mssp.2021.106097

Kumar, N., Irfan, G., Udayabhanu, G. and Nagaraju, Green synthesis of zinc oxide nanoparticles: Mechanical and microstructural characterization of aluminum nano composites, *Mater. Today Proc.*, 38(5), 3116-3124 (2021). https://doi.org/10.1016/j.matpr.2020.09.494

Kumar, S., Singh, A., Singh, R., Singh, S., Kumar, P. and Kumar, R., Facile h-MoO_3 synthesis for NH_3 gas sensing application at moderate operating temperature, *Sens Actuators B Chem.*, 325, 128974 (2020). https://doi.org/10.1016/j.snb.2020.128974

Rajesh, E. M., Shamili, K., Rajendran, R., Shankar, S. R. and Elango, M., Superparamagnetic Nanoparticles of Iron Oxide: Synthesis and Characterization, *ASEM.*, 6 (3), 268-272 (2014). https://doi.org/10.1166/asem.2014.1503

Tariq, N., Fatima, R., Rahman, A., Zulfqar, S., Warsi, M.F. and Shakir, I., Synthesis and characterization of $MoO_3/CoFe_2O_4$ nanocomposite for photocatalytic applications. *Ceram. Int.*, 46, 21596–21603 (2020). https://doi.org/10.1016/j.ceramint.2020.05.264

Wang, J., Nie, X., Wang, W., Zhao, Z., Li, L. and Zhang, Z., Single-layer graphene-TiO_2 nanotubes array heterojunction as photoanode to enhance the photoelectric of DSSCs, *Optik*, 242, 167245 (2021). https://doi.org/10.1016/j.ijleo.2021.167245

Xu, H., Liu, C., Srinivasakannan, C., Chen, M., Wang, Q., Li, L. and Dai, Y., Hydrothermal synthesis of one-dimensional α-MoO_3 nanomaterials and its unique sensing mechanism for ethanol, *Arab. J. Chem.*, 15(9), 104083 (2022). https://doi.org/10.1016/j.arabjc.2022.104083

Zhou, L., Mi, Q., Jin, Y. Tingting, Li. and Dongzhi, Z. Construction of $MoO_3/MoSe_2$ nanocomposite-based gas sensor for low detection limit trimethylamine sensing at room temperature, *J. Mater. Sci: Mater Electron.*, 32, 17301–17310(2021). https://doi.org/10.21203/rs.3.rs-336116/v1